Electronic Supplementary Material (ESI) for Materials Chemistry Frontiers.

Supporting Information

Novel Ordered Hollow Spherical Nickel Silicate-Nickel Hydroxide United Composite with Two Types of Morphologies for Enhanced Electrochemical Storage Performance

Qiushi Wang, Yifu Zhang*, Jinqiu Xiao, Hanmei Jiang, Xiaojuan Li, Changgong Meng

School of Chemical Engineering, Dalian University of Technology, Dalian 116024, PR China

*Corresponding author. E-mail address: yfzhang@dlut.edu.cn

Preparation of $Ni(OH)_2$

In a typical synthesis of the layered $Ni(OH)_2$, 5.8 mmol $Ni(NO_3)_2 \cdot 6H_2O$ was dissolved in 18 mL deionized water under constant stirring. Then, 5 mmol NH_4Cl and 1 mL $NH_3 \cdot H_2O$ was dissolved in 20 mL deionized water under constant stirring. After the solutions are mixed, a further stirring for 30 min is in process. The final mixture was transferred into a 50 mL Teflon-lined stainless autoclave and treated at 120 °C for 20 h. The result product was cooled down to room temperature and collected by filtration, then washed with water and ethanol three times repeatedly. Finally, the product was dried at 60 °C for 12 h before used.

Preparation of NiSiOx

0.1 g SiO_2 sphere was dispersed into 18 mL deionized by ultrasonication. 3.7 mmol $NiCl_2 \cdot 6H_2O$, 12 mmol NH_4Cl, 0.24 mL $NH_3 \cdot H_2O$ was added into 20 mL deionized water under vigorously stirring. The two solutions were mixed and continuous stirred for another 10 min. Then, a hydrothermal treatment was carried by transferred the mixture into a Teflon-lined stainless-steel autoclave and heated at 120 °C for 20 h. Finally, the products were collected by centrifugation and washed with deionized water and ethanol 3 times repeatedly, along with vacuum dried at 60 °C for 12 h.

Figure S1

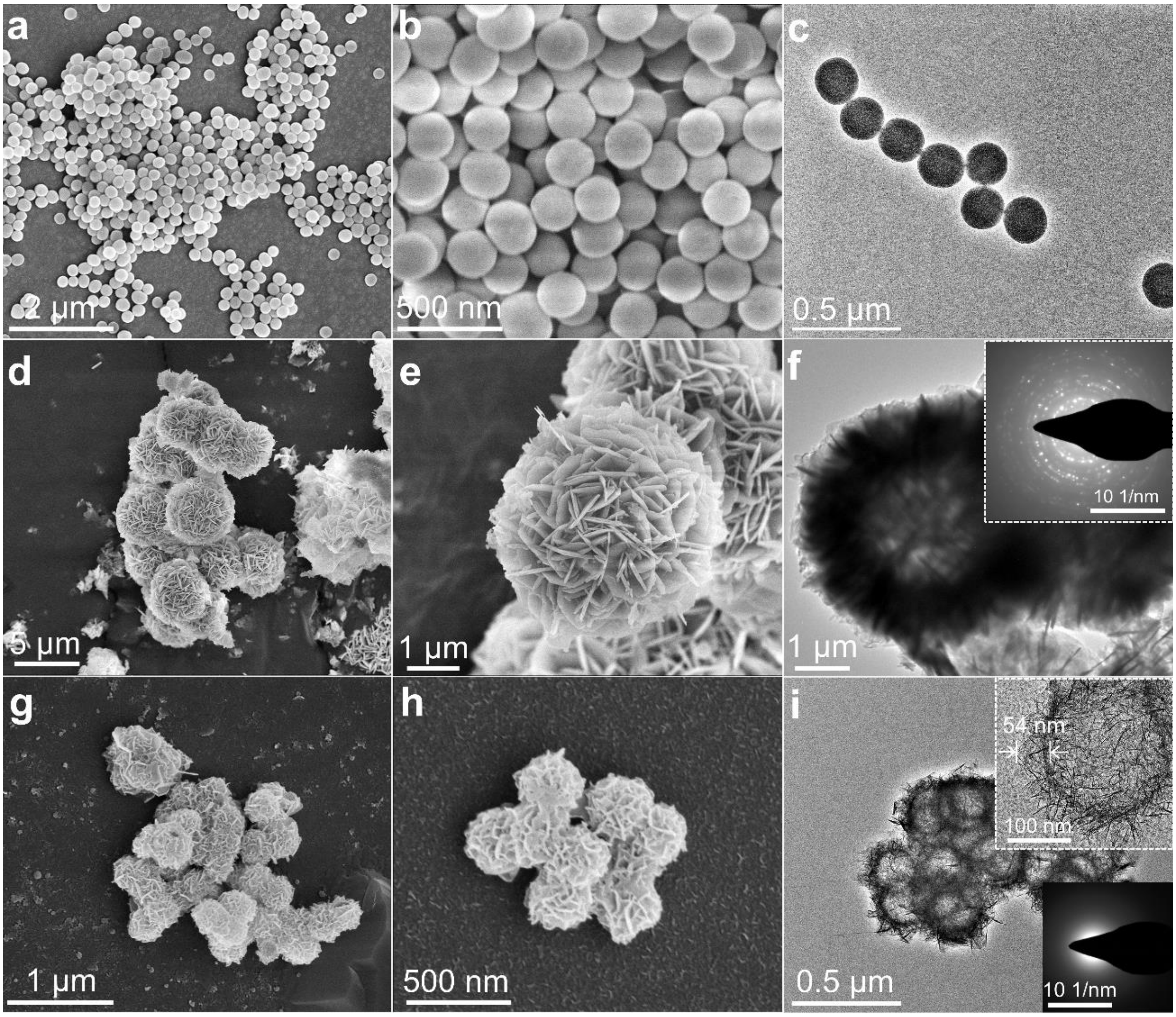

Figure S1. (a-b)(d-e)(g-h) FE SEM images of the SiO_2 sphere, $Ni(OH)_2$ and NiSiOx. (c, f, i) TEM images of SiO_2 sphere, $Ni(OH)_2$ and NiSiOx. The insets in (f) and (i) are the SAED patterns of $Ni(OH)_2$ and NiSiOx.

Figure S2

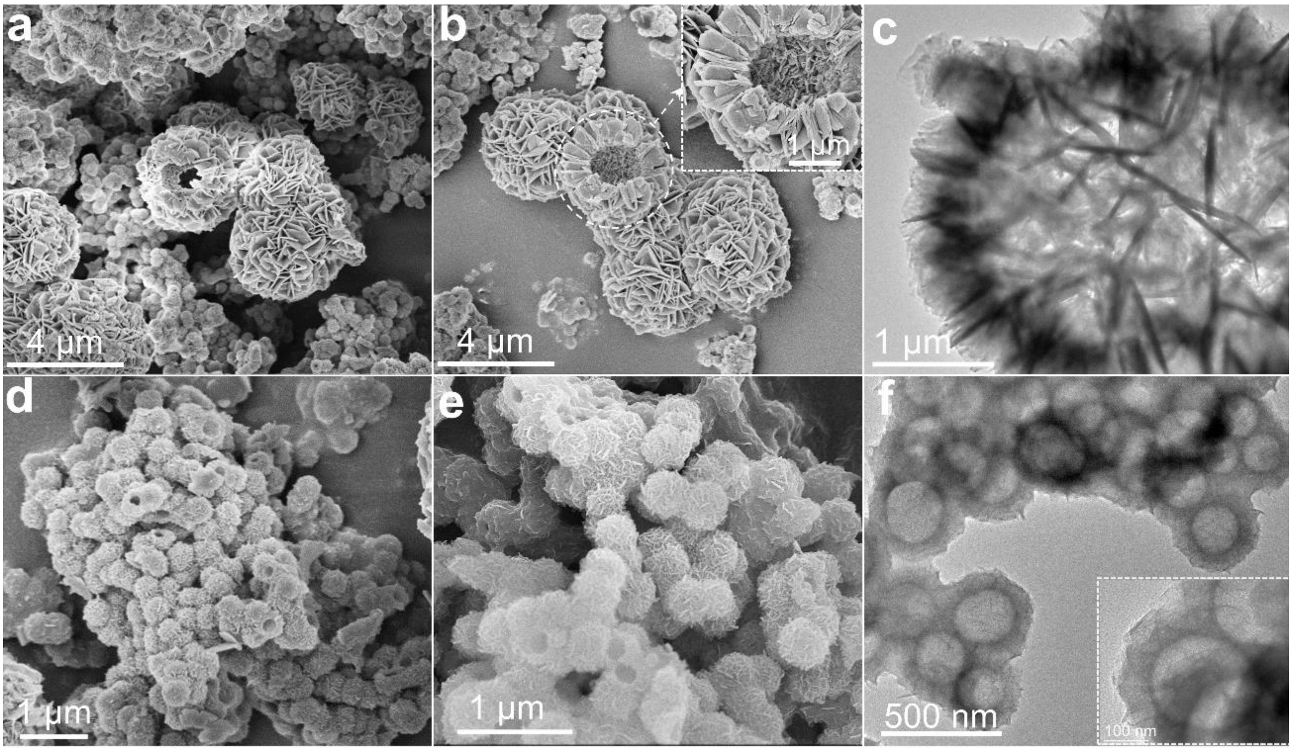

Figure S2. (a-b) FE SEM images of the $Ni(OH)_2$-Si in NiSi-$Ni(OH)_2$-4. (c)TEM image of the $Ni(OH)_2$-Si in NiSi-$Ni(OH)_2$-4. (d-e) FE SEM images of the $Ni(OH)_2$@NiSi in NiSi-$Ni(OH)_2$-4. (f) TEM image of the $Ni(OH)_2$@NiSi in NiSi-$Ni(OH)_2$-4.

Figure S3

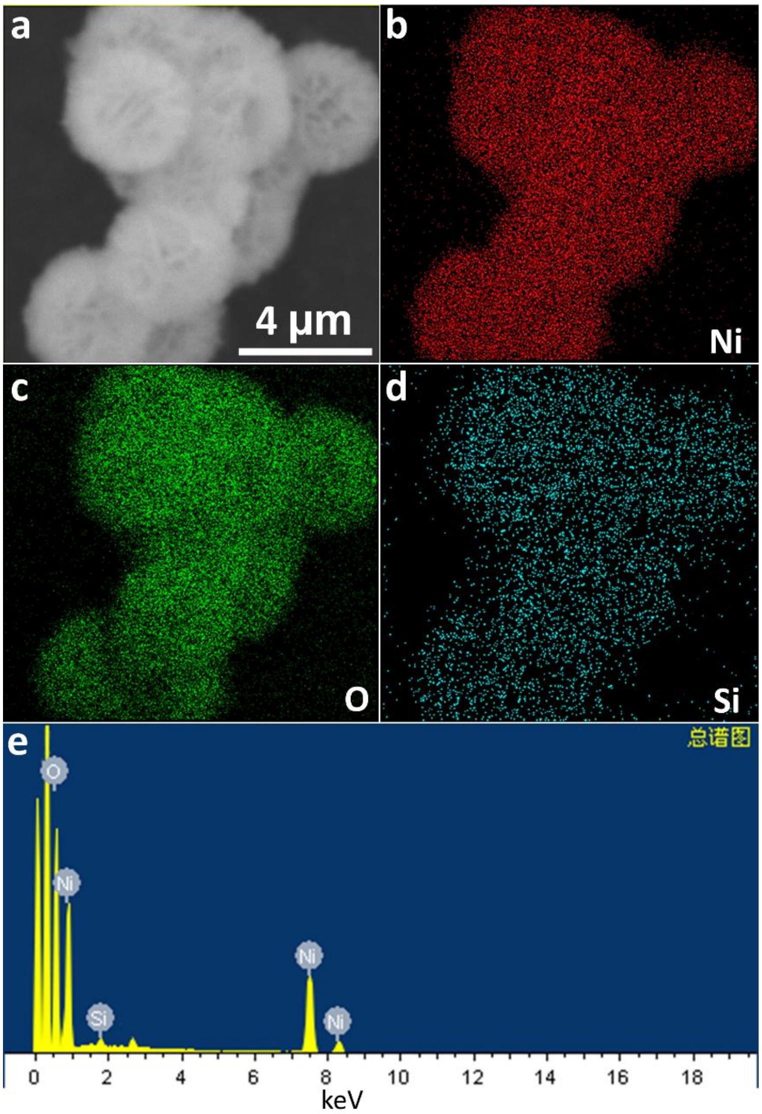

Figure S3. The selected SEM area (a), Elemental mapping images of (b) Ni, (c) O, (d) Si elements and EDX spectrum (e) of $Ni(OH)_2$-Si in NiSi-$Ni(OH)_2$-4.

Figure S4

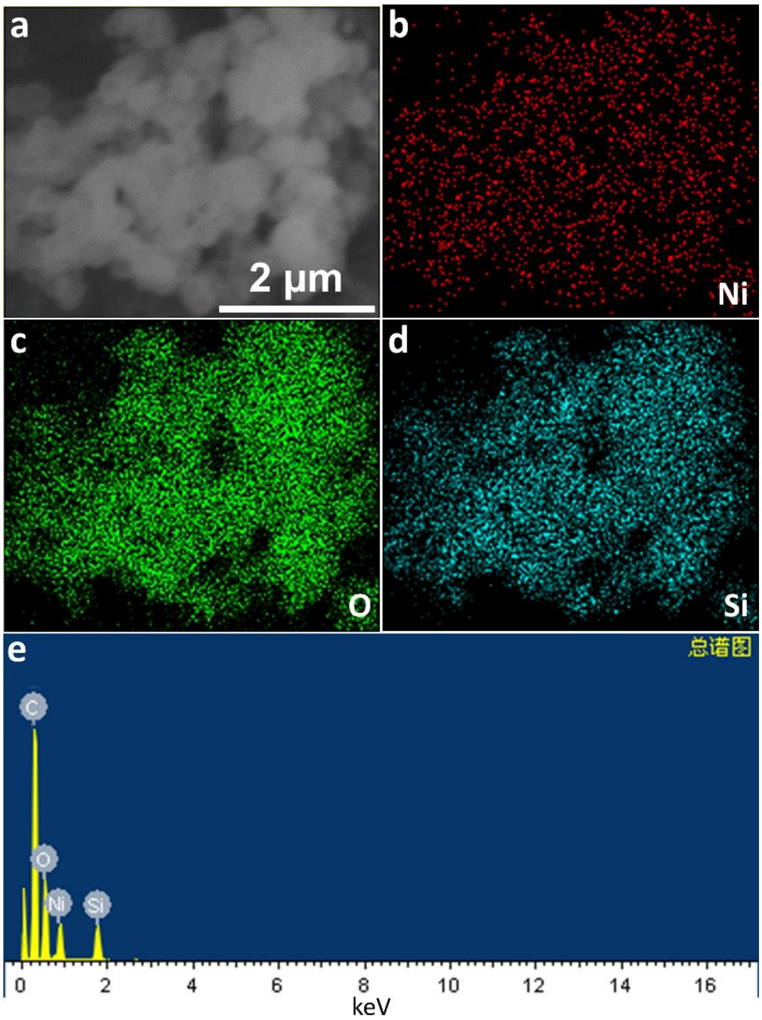

Figure S4. The selected SEM area (a), Elemental mapping images of (b) Ni, (c) O, (d) Si elements and EDX spectrum (e) of NiSi@$Ni(OH)_2$ in NiSi-$Ni(OH)_2$-4.

Figure S5

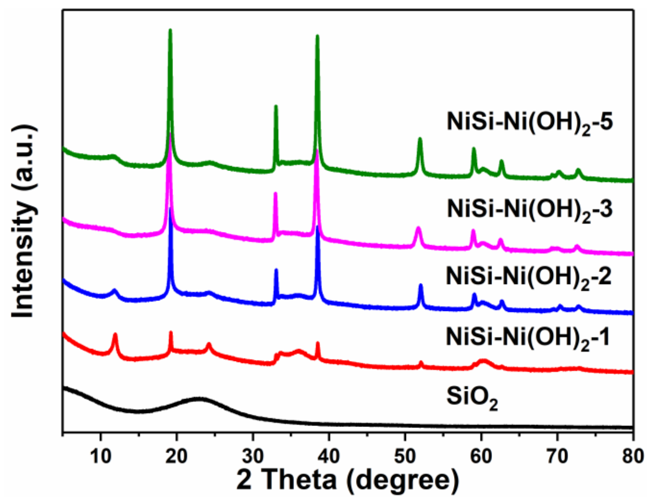

Figure S5. XRD patterns of SiO_2, NiSi-Ni$(OH)_2$-1~3 and NiSi-Ni$(OH)_2$-5.

Figure S6

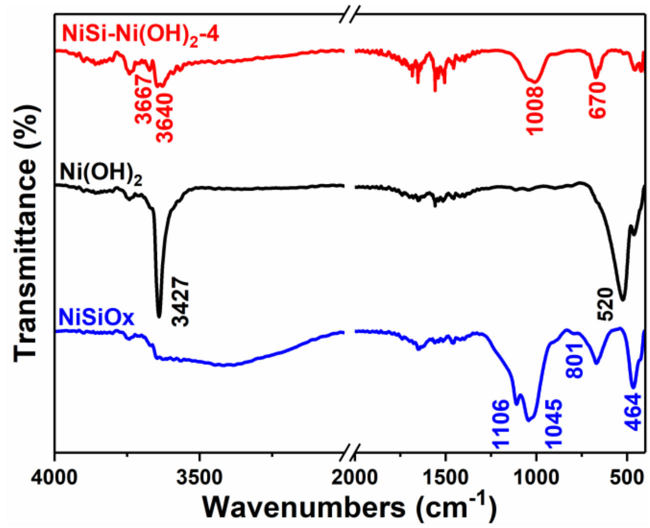

Figure S6. FT IR spectra of NiSiOx, $Ni(OH)_2$ and NiSi-$Ni(OH)_2$-4.

Figure S7

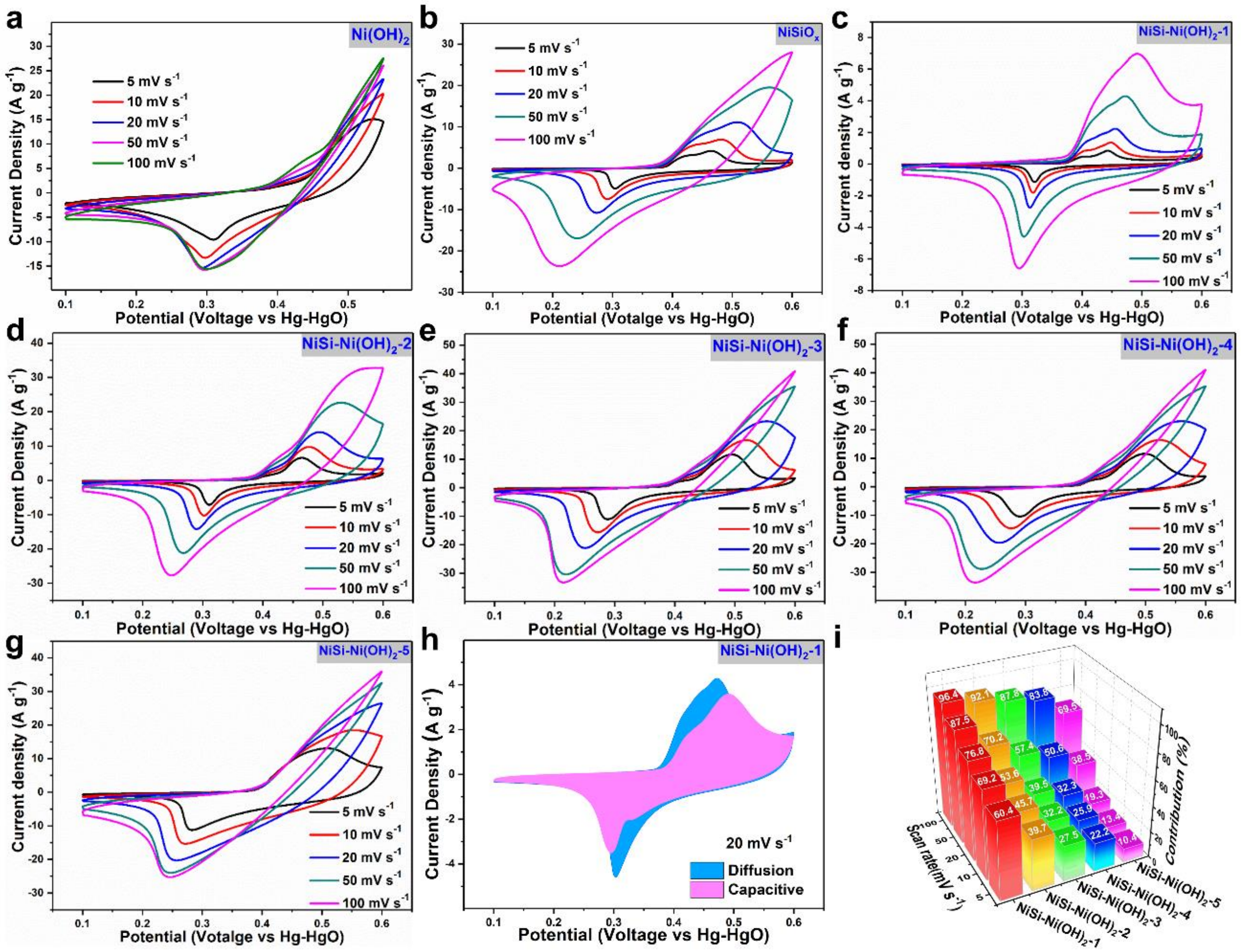

Figure S7. CV curves of (a) $Ni(OH)_2$, (b) NiSiOx and (c-g) NiSi-$Ni(OH)_2$-1~5 at different scan rates (5, 10, 20, 50 and 100 mV s^{-1}).(h) Capacitive and diffusion-controlled contributions at 20 mV s^{-1} of NiSi-$Ni(OH)_2^{-1}$. (i) Capacitive contribution at different scan rates of NiSi-$Ni(OH)_2$-1~5.

Figure S8

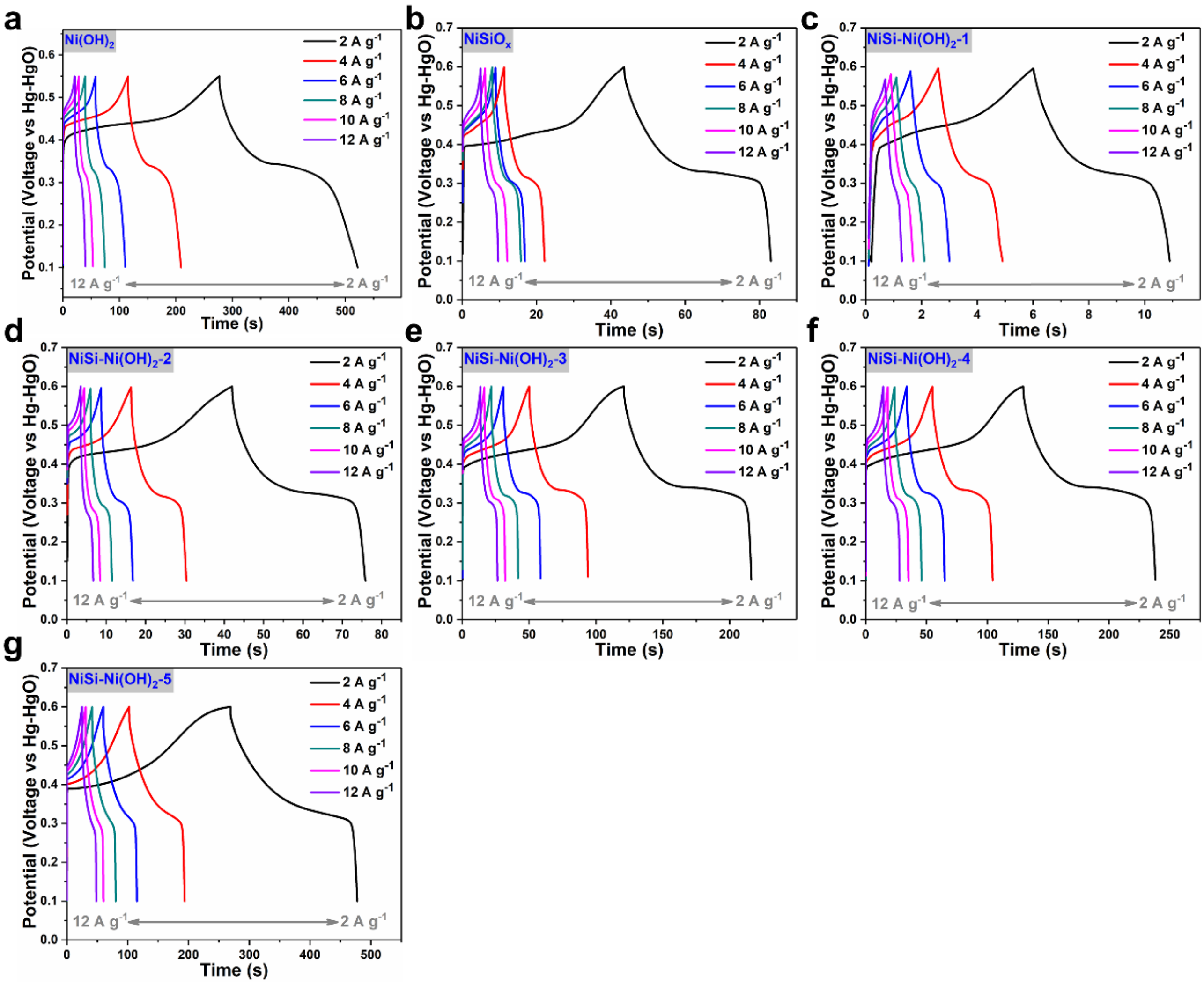

Figure S8. GCD curves of (a) $Ni(OH)_2$, (b) NiSiOx and (c-h) NiSi-$Ni(OH)_2$-1~5 at different discharge currents (2, 4, 6, 8, 10 and 12 A g^{-1}).

Figure S9

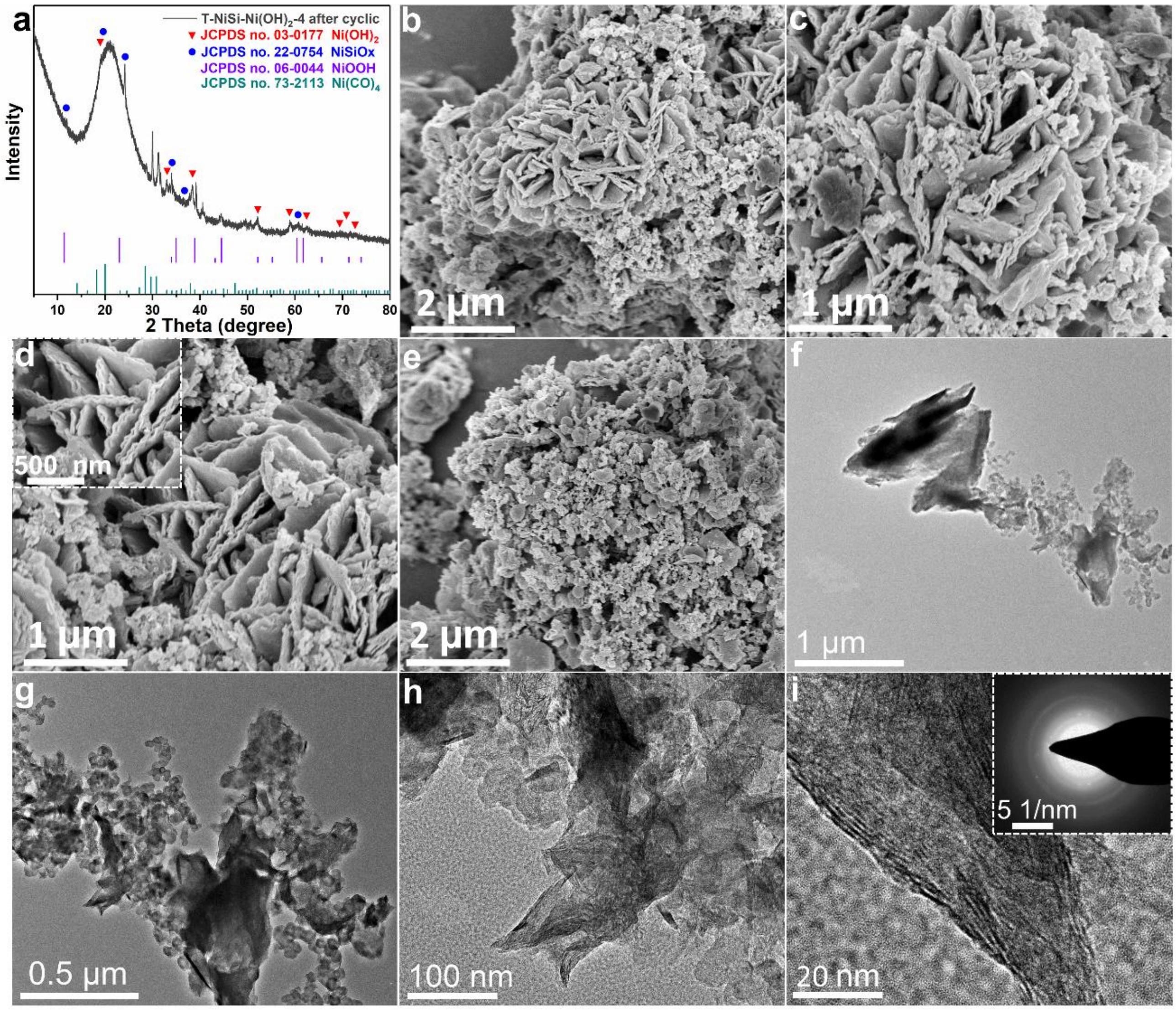

Figure S9. (a) XRD patterns of NiSi-Ni(OH)$_2$-4 after cycling. (b-e) FE-SEM images of NiSi-Ni(OH)$_2$-4 after cycling. (f-i) TEM and HR-TEM images of NiSi-Ni(OH)$_2$-4 after cycling. (h-i) FE-SEM images of NiSi after cycling.

Figure S10

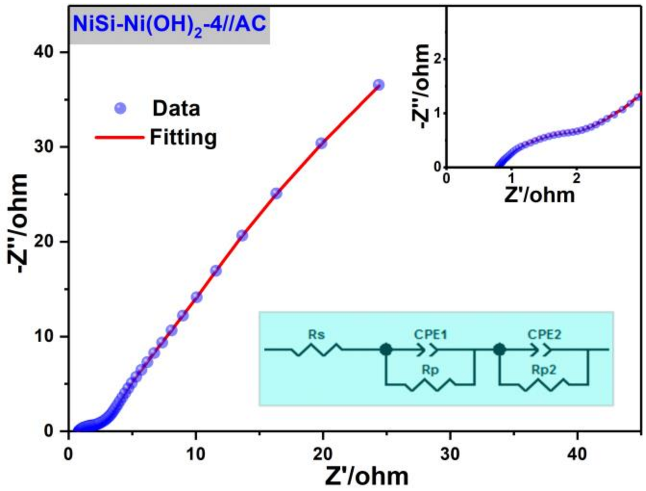

Figure S10. Nyquist plots of the HSC. The insets are the enlarged Nyquist plot from the high-frequency region and the equivalent circuit for the electrochemical impedance spectrum.

Table S1

Table S1. Comparison of the electrochemical performance with work from literatures based on nickel silicate/nickel hydroxide-based materials.

Nickel silicate/nickel hydroxide-based materials	Electrolyte	Potential /V	Capacitance	Cycle	Ref.
(Ni, Co)$_3$Si$_2$O$_5$(OH)$_4$	1 M KOH	0~0.5	144 F g^{-1}, 1 A g^{-1}	99.3%, 10000 cycles	1
Ni$_3$Si$_2$O$_5$(OH)$_4$	6 M KOH	0~0.5	887 F g^{-1}, 0.7 A g^{-1}	96.8%, 2000 cycles	2
Ni$_3$Si$_2$O$_5$(OH)$_4$/RGO	2 M KOH	0.2~0.6	178.9 F g^{-1}, 1 A g^{-1}	97.6%, 5000 cycles	1
C/Ni$_3$Si$_2$O$_5$(OH)$_4$	3 M KOH	−1~−0.3	132.4 F·g^{-1}, 0.5 A·g^{-1}	100%, 10000 cycles	3
Ni$_3$Si$_2$O$_5$(OH)$_4$/rGO microspheres	2M KOH	0.15~0.65	178.9F·g^{-1}, 1 A·g^{-1}	97.6%,5000 cycles	1
NiSi hollow sphere	3 M KOH	0~0.6	66.7 F g^{-1}, 0.5 A g^{-1}	44%, 5000 cycles	4
NG/Ni(OH)$_2$	2 M KOH	0~0.5	782 F g^{-1}, 0.2 A g^{-1}	90%, 10000 cycles	5
Nickel hydroxide	1 M KOH	0.1~0.6	3637 F g^{-1}, 1 A g^{-1}	80%, 10000 cycles	6
β-Ni(OH)$_2$	6 M KOH	0.1~0.55	2537.4 F g^{-1}, 1 A g^{-1}	77.6%, 3000 cycles	7
Ni(OH)$_2$ nanosheets	2 M KOH	0~0.45	2384.3 F g^{-1}, 1 A g^{-1}	75%, 3000 cycles	8
Ni(OH)$_2$-PPy	3 M KOH	0~0.5	352 F g^{-1}, 1 A g^{-1}	87%, 7000 cycles	9
Ni(OH)$_2$–POV	2 M KOH	0~0.45	1440 F g^{-1}, 1 A g^{-1}	85%, 2000 cycles	10
Ni(OH)$_2$ nanotubes	6 M KOH	−0.15~0.45	1319 F g^{-1}, 3 A g^{-1}	79.3%, 7000 cycles	11
Nickel hydroxide–nickel	3 M KOH	0~0.5	1793 F g^{-1}, 1.25 A g^{-1}	97.2%, 3000 cycles	12
Nickel hydroxide	1 M KOH	0~0.5	2801 F g^{-1}, 2 A g^{-1}	83%, 1500 cycles	13
HCNs@NiCo-LDH	6 M KOH	0~0.6	2558 F g^{-1}, 1 A g^{-1}	77%, 10000 cycles	14
Ag NW/Ni(OH)$_2$	1 M KOH	0~0.6	164.8 F g^{-1}, 5 mV s^{-1}	62.5%, 1000 cycles	15
Ni1Co2	3 M KOH	0~0.45	2654.9 F g^{-1}, 1 A g^{-1}	77%, 1500 cycles	16
CNT@Ni(OH)$_2$	1 M KOH	0~0.5 V	1136 F g^{-1} at 2 A g^{-1}	92%, 1000 cycles	17
NiSi-Ni(OH)$_2$	3M KOH	0.1~0.6	476.4 F·g^{-1}, 2 A·g^{-1}	103.3%, 10000 cycles	This work

References

1. Y. Zhang, W. Zhou, H. Yu, T. Feng, Y. Pu, H. Liu, W. Xiao and L. Tian, *Nanoscale Res. Lett.*, 2017, **12**, 325.
2. J. Zhao, Y. Zhang, T. Wang, P. Li, C. Wei and H. Pang, *Adv. Mater. Interfaces*, 2015, **2**, 1400377.
3. Q. Wang, Y. Zhang, H. Jiang, T. Hu and C. Meng, *ACS Appl. Energy Mater.*, 2018, **1**, 3396-3409.
4. Q. Wang, Y. Zhang, H. Jiang, X. Li, Y. Cheng and C. Meng, *Chem. Eng. J.*, 2019, **362**, 818-829.
5. L. Mao, C. Guan, X. Huang, Q. Ke, Y. Zhang and J. Wang, *Electrochim. Acta*, 2016, **196**, 653-660.
6. S.-W. Kim, I.-H. Kim, S.-I. Kim and J.-H. Jang, *Chemistry – An Asian Journal*, 2017, **12**, 1291-1296.
7. X. Hu, S. Liu, C. Li, J. Huang, J. Luv, P. Xu, J. Liu and X.-Z. You, *Nanoscale*, 2016, **8**, 11797-11802.
8. X. Xiong, D. Ding, D. Chen, G. Waller, Y. Bu, Z. Wang and M. Liu, *Nano Energy*, 2015, **11**, 154-161.
9. W. He, G. Zhao, P. Sun, P. Hou, L. Zhu, T. Wang, L. Li, X. Xu and T. Zhai, *Nano Energy*, 2019, **56**, 207-215.
10. J. L. Gunjakar, A. I. Inamdar, B. Hou, S. Cha, S. M. Pawar, A. A. Abu Talha, H. S. Chavan, J. Kim, S. Cho, S. Lee, Y. Jo, H. Kim and H. Im, *Nanoscale*, 2018, **10**, 8953-8961.
11. Y. Wang, B. Shang, F. Lin, Y. Chen, R. Ma, B. Peng and Z. Deng, *Chem. Commun.*, 2018, **54**, 559-562.
12. J. Zhao, J. He, M. Sun, M. Qu and H. Pang, *Inorg. Chem. Front.*, 2015, **2**, 129-135.
13. L. Zhang, T. J. Huang and H. Gong, *Phys. Chem. Chem. Phys.*, 2017, **19**, 10462-10469.
14. J. Xu, C. Ma, J. Cao and Z. Chen, *Dalton Trans.*, 2017, **46**, 3276-3283.
15. H. Du, Y. Pan, X. Zhang, F. Cao, T. Wan, H. Du, R. Joshi and D. Chu, *Nanoscale Advances*, 2019, **1**, 140-146.
16. L. Ye, L. Zhao, H. Zhang, B. Zhang and H. Wang, *J. Mater. Chem. A*, 2016, **4**, 9160-9168.
17. H. Yi, H. Wang, Y. Jing, T. Peng, Y. Wang, J. Guo, Q. He, Z. Guo and X. Wang, *J. Mater. Chem. A*, 2015, **3**, 19545-19555.